Article

Cell Reports

The Histone Variant MacroH2A1.2 Is Necessary for the Activation of Muscle Enhancers and Recruitment of the Transcription Factor Pbx1

Graphical Abstract

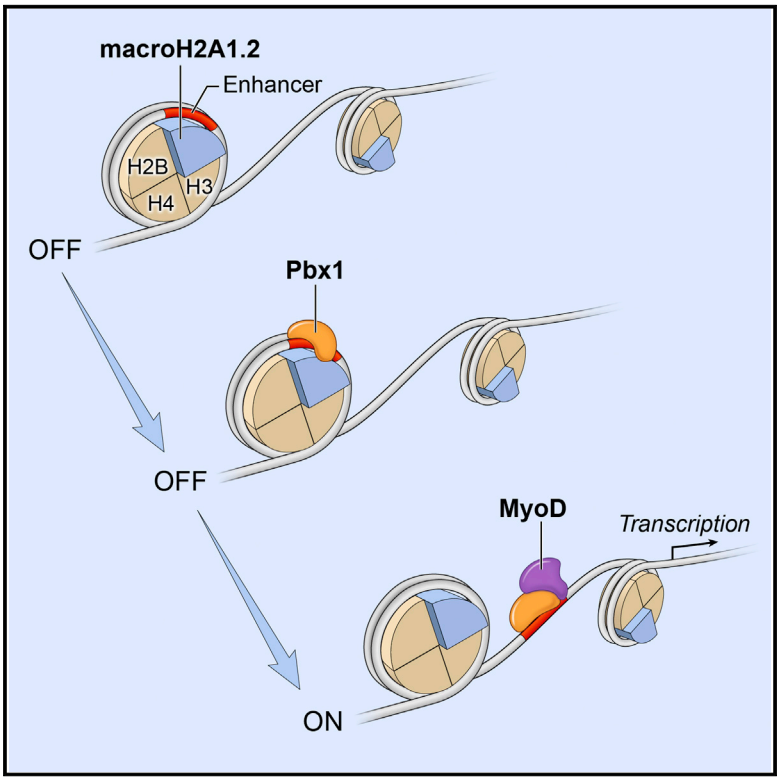

Authors

Stefania Dell'Orso, A. Hongjun Wang, Han-Yu Shih, ..., John J. O'Shea, Vittorio Sartorelli, Hossein Zare

Correspondence

sartorev@mail.nih.gov

In Brief

Dell'Orso et al. report that the histone variant macroH2A1.2 is required for activation of muscle-gene expression and cell differentiation. Genome-wide analyses indicate that macroH2A1.2 is enriched at prospective muscle-specific enhancers where it is required for H3K27 acetylation and recruitment of the transcription factor Pbx1.

Highlights

- MacroH2A1.2 is enriched at prospective muscle-specific enhancers
- Activation of muscle-specific enhancers requires macroH2A1.2
- MacroH2A1.2 is required for the activation of the myogenic regulatory network
- Recruitment of Pbx1 at muscle regulatory regions is contingent on macroH2A1.2

Accession Numbers

GSE76010

Dell'Orso et al., 2016, Cell Reports *14*, 1156–1168
February 9, 2016
http://dx.doi.org/10.1016/j.celrep.2015.12.103

OPEN ACCESS
CellPress

Cell Reports
Article

The Histone Variant MacroH2A1.2 Is Necessary for the Activation of Muscle Enhancers and Recruitment of the Transcription Factor Pbx1

Stefania Dell'Orso,[1] A. Hongjun Wang,[1] Han-Yu Shih,[2] Kayoko Saso,[1] Libera Berghella,[3] Gustavo Gutierrez-Cruz,[1] Andreas G. Ladurner,[4] John J. O'Shea,[2] Vittorio Sartorelli,[1,*] and Hossein Zare[1]

[1]Laboratory of Muscle Stem Cells and Gene Regulation, National Institute of Arthritis and Musculoskeletal and Skin Diseases (NIAMS), NIH, Bethesda, MD 20892, USA
[2]Lymphocyte Cell Biology Section, Molecular Immunology and Inflammation Branch, NIAMS, NIH, Bethesda, MD 20892, USA
[3]Epigenetics and Regenerative Medicine, IRCCS Fondazione Santa Lucia, 00143 Rome, Italy
[4]Butenandt Institute, LMU Biomedical Center, Department of Physiological Chemistry, Ludwig-Maximilians-University of Munich, 81377 Munich, Germany
*Correspondence: sartorev@mail.nih.gov
http://dx.doi.org/10.1016/j.celrep.2015.12.103

SUMMARY

Histone variants complement and integrate histone post-translational modifications in regulating transcription. The histone variant macroH2A1 (mH2A1) is almost three times the size of its canonical H2A counterpart, due to the presence of an ~25 kDa evolutionarily conserved non-histone macro domain. Strikingly, mH2A1 can mediate both gene repression and activation. However, the molecular determinants conferring these alternative functions remain elusive. Here, we report that mH2A1.2 is required for the activation of the myogenic gene regulatory network and muscle cell differentiation. H3K27 acetylation at prospective enhancers is exquisitely sensitive to mH2A1.2, indicating a role of mH2A1.2 in imparting enhancer activation. Both H3K27 acetylation and recruitment of the transcription factor Pbx1 at prospective enhancers are regulated by mH2A1.2. Overall, our findings indicate a role of mH2A1.2 in marking regulatory regions for activation.

INTRODUCTION

Histone post-translational modifications shape the epigenome and regulate transcription (Jenuwein and Allis, 2001; Kundaje et al., 2015). The nucleosome incorporation of histone variants provides an additional regulatory layer that influences the formation of chromatin states associated with either transcriptional repression or activation (Jin and Felsenfeld, 2007; Jin et al., 2009; Barski et al., 2007; Maze et al., 2014). Localized replacement of canonical histones by histone variants modifies the chromatin structure to attract or repel transcription factors, chromatin writers, readers, and erasers (Skene and Henikoff, 2013). Among the different histone variants, the two isoforms macroH2A1.1 and -1.2 are characterized by the presence of an evolutionarily conserved, ~25-kDa carboxyl-terminal globular region called the macro domain (Pehrson and Fried, 1992), serving as surface for interaction with metabolites and histone modifiers (Ladurner, 2003; Kustatscher et al., 2005; Chakravarthy et al., 2005; Gamble and Kraus, 2010; Hussey et al., 2014). A role for mH2A1 in mediating gene repression was initially suggested by observations linking it to female X chromosome inactivation (Costanzi and Pehrson, 1998; Csankovszki et al., 2001). More recently, mH2A1 has been shown to contrast reprogrammed pluripotency (Gaspar-Maia et al., 2013; Barrero et al., 2013; Pasque et al., 2011), to repress expression of the *HoxA* cluster (Buschbeck et al., 2009) and of the α-globin locus in erythroleukemic cells (Ratnakumar et al., 2012), and to suppress melanoma progression through regulation of cyclin-dependent protein kinase (CDK)8 (Kapoor et al., 2010). However, there is evidence to suggest that mH2A1 has a multifaceted function in controlling gene transcription (Gamble et al., 2010). Reducing mH2A1 levels not only does not result in generalized de-repression of mH2A1-bound genes but is, in fact, associated with failure to activate up to 75% of its targets (Gamble et al., 2010). Moreover, while inhibiting p300-dependent histone acetylation in vitro (Doyen et al., 2006), mH2A1 has been recently reported to cooperate with PARP-1 to regulate transcription by promoting CBP (CREB-binding protein)-mediated acetylation of histone H2B at lysines 12 and 120, with opposing effects on transcription (Chen et al., 2014). These and other observations (Creppe et al., 2012; Podrini et al., 2014) indicate that mH2A1 may exert a dual function in regulating gene expression.

Here, we report that mH2A1.2 is involved in imparting enhancer competency in skeletal muscle cells. In agreement with previous findings, mH2A1.2 was localized to the H3K27me3 promoter regions of repressed genes. However, mH2A1.2-occupied and -repressed targets were not reactivated upon mH2A1.2 knockdown. Instead, activation of muscle enhancers was dependent on mH2A1.2, as its reduction brought about decreased H3K27 acetylation. Reducing mH2A1.2 impaired expression of the master developmental regulator *Myogenin*, resulting in defective activation of the myogenic gene regulatory network and

muscle cell differentiation. Notably, mH2A1.2 mediated chromatin engagement of Pbx1, a homeodomain transcription factor priming MyoD gene targets for activation (Berkes et al., 2004; Maves et al., 2007). In aggregate, these findings assign a role to mH2A1.2 in conferring enhancer marking and activation via regulation of transcription factors' recruitment and H3K27 acetylation.

RESULTS

Genome-wide Distribution of the Histone Variant MacroH2A1.2 Reveals Preferential Association with Regions of Active Transcription

To investigate the role of the histone variant mH2A1 in transcriptional regulation of cell differentiation, we used the mouse skeletal muscle C2C12 cell line, as a model system. C2C12 cells recapitulate muscle differentiation in culture, as they can be kept in an undifferentiated state as myoblasts (MBs) and induced to differentiate to form multinucleated myotubes (MTs) (Yaffe and Saxel, 1977). Both alternatively spliced mH2A1.1 and 1.2 isoforms (Rasmussen et al., 1999; Costanzi and Pehrson, 2001) were expressed in C2C12 cells (Figure S1A). Since RNA sequencing (RNA-seq) analysis indicated that the mH2A1.2 isoform was the most represented in MBs and expressed at levels similar to those of mH2A1.1 in MTs (Figure S1B), we chose to focus our study on the mH2A1.2 isoform. Analysis of chromatin immunoprecipitation sequencing (ChIP-seq) data generated from two experiments with two different mH2A1.2 antibodies (see Experimental Procedures) identified ~77,000 overlapping enriched genomic regions in MBs and ~36,600 in MTs, respectively (Figures S1C and S1D; Table S1). Peak calling with either the MACS2 (Feng et al., 2012) or the SICER (Zang et al., 2009) algorithm identified largely overlapping mH2A1.2-enriched regions (Figure S1E). Examples of mH2A1.2-occupied regions, as called by the MACS2 algorithm, are illustrated in Figure S1F. A global reduction of the mH2A1.2 signal was observed after mH2A1.2 knockdown, indicating that the majority of peaks correspond to the mH2A1.2 isoform (Figures S1G and S1H).

Genome-wide distribution of mH2A1.2 was similar in MBs and MTs (Figure 1A). Genome-wide maps of mH2A1.2, intersected with those of active and repressive epigenetic marks in MBs, revealed that the majority of mH2A1.2 peaks was localized at active regions (Figure 1B). Specifically, 32% of mH2A1.2 peaks occurred at H3K4me1$^+$/H3K27ac$^+$ regions (active enhancers), 21% occurred at H3K4me1$^+$ regions, 19% overlapped with H3K4me3$^+$/H3K27ac$^+$ (active promoters), and 25% of mH2A1.2 peaks were located at regions not occupied by any of the aforementioned epigenetic marks considered (mH2A1.2 only). In contrast, only 3% of mH2A1.2 peaks co-localized with the repressive mark H3K27me3 (Figure 1B). Furthermore, among mH2A1.2-bound promoters, only 8% were H3K27me3$^+$, while 67% of these promoters were occupied by both H3K4me3 and H3K27ac (Figure S2A). In MTs, the percentage of mH2A1.2$^+$/H3K27me3$^+$ regions increased to 18% (Figure 1B), and a Gene Ontology (GO) analysis of the newly acquired mH2A1.2$^+$/H3K27me3$^+$ TSS (transcription start site) identified terms related to, among others, "neuron differentiation," " pattern specification process," and "embryonic morphogenesis" (Table S1). Reduction of mH2A1.2 peaks at active enhancers (32% in MB versus 7% in MT; Figure 1B) occurred at MT-specific enhancers (i.e., enhancers active in MT; discussed later) (Figure S2B) and coincided with increased mH2A1.2 occupancy at H3K4me1$^+$ and otherwise non-epigenetically defined genomic regions (64%; Figure 1B). mH2A1.2 occupancy was also reduced, but more modestly, at constitutive enhancers (i.e., enhancers active in both MB and MT; discussed later) in MTs (Figure S2C).

Examples of expressed genes occupied by mH2A1.2 are shown in Figure 1C. Developmental regulators of other cell lineages, such as *Neurog2* and *Wnt1*, which are transcriptionally silent in C2C12 cells (Mousavi et al., 2012), are among mH2A1.2-bound genes with H3K27me3 (Figure 1D).

We assigned MB-mH2A1.2$^+$ active enhancers or MB-mH2A1.2$^+$ regions acquiring either H3K4me1$^+$ or H3K4me1$^+$/H3K27ac$^+$ in MTs to genes by proximity (Whyte et al., 2013; Mousavi et al., 2013) and queried gene expression changes occurring during the transition from MB to MT. Enhancers residing within 100 kb, 50 kb, or 20 kb from the closest promoter were considered. While the number of enhancer-assigned genes increased with increasing genomic intervals (Figure S2D), GO analyses for 100-kb and 50-kb intervals captured essentially all the terms returned by the analysis conducted for the 20-kb interval, including "muscle cell differentiation" and "muscle and muscle system process" (Figure S2E; Table S1). Therefore, for further analysis, we considered a proximity measure of 20 kb to assign genes to identified enhancers. Genomic regions that became active enhancers in MT displayed a clear association with upregulated genes (Figure 1E). Similarly, a smaller set comprising genes assigned to mH2A1.2$^+$ regions and occupied by H3K4me1 and H3K27me3 marks in MBs was also enriched for upregulated genes in MTs (Table S2). Overall, these results indicate that mH2A1.2 preferentially occupies transcriptionally active genomic regions in MB or regions programmed to be activated in MT.

MacroH2A1.2 Is Required for the Activation of the Myogenic Gene Regulatory Network and Differentiation of Skeletal Muscle Cells

We addressed the function of mH2A1.2 during muscle cell differentiation by transfecting C2C12 cells with either control or two different mH2A1.2 small interfering RNAs (siRNAs; mH2A1.2 interference, mH2A1.2i) (Figure 2A; Figure S3A) and inducing them to differentiate to form MTs. For further analysis, we chose to use mH2A1.2i_2 siRNAs, as they were the most effective (Figure S3A). mH2A1.2 siRNA specifically reduced mH2A1.2 but not the closely related mH2A1.1 isoform (Figure S3B). MB growth was not affected by mH2A1.2i (Figure S3C). However, Myogenin, a myogenic transcription factor required for muscle differentiation (Tapscott, 2005), was reduced (Figures 2A–2C; Figures S3A and S3D), and formation of muscle-specific myosin-heavy-chain (MHC)-positive, multinucleated MTs was compromised by mH2A1.2i (Figure 2D). The expression of the muscle-specific gene troponin T type 1 (Tnnt1) was also greatly reduced (Figure S3E). To complement knockdown experiments, exogenous FLAG-tagged mH2A1.2 was expressed in C2C12 cells and found to increase *Myogenin* expression (Figures 2E and 2F).

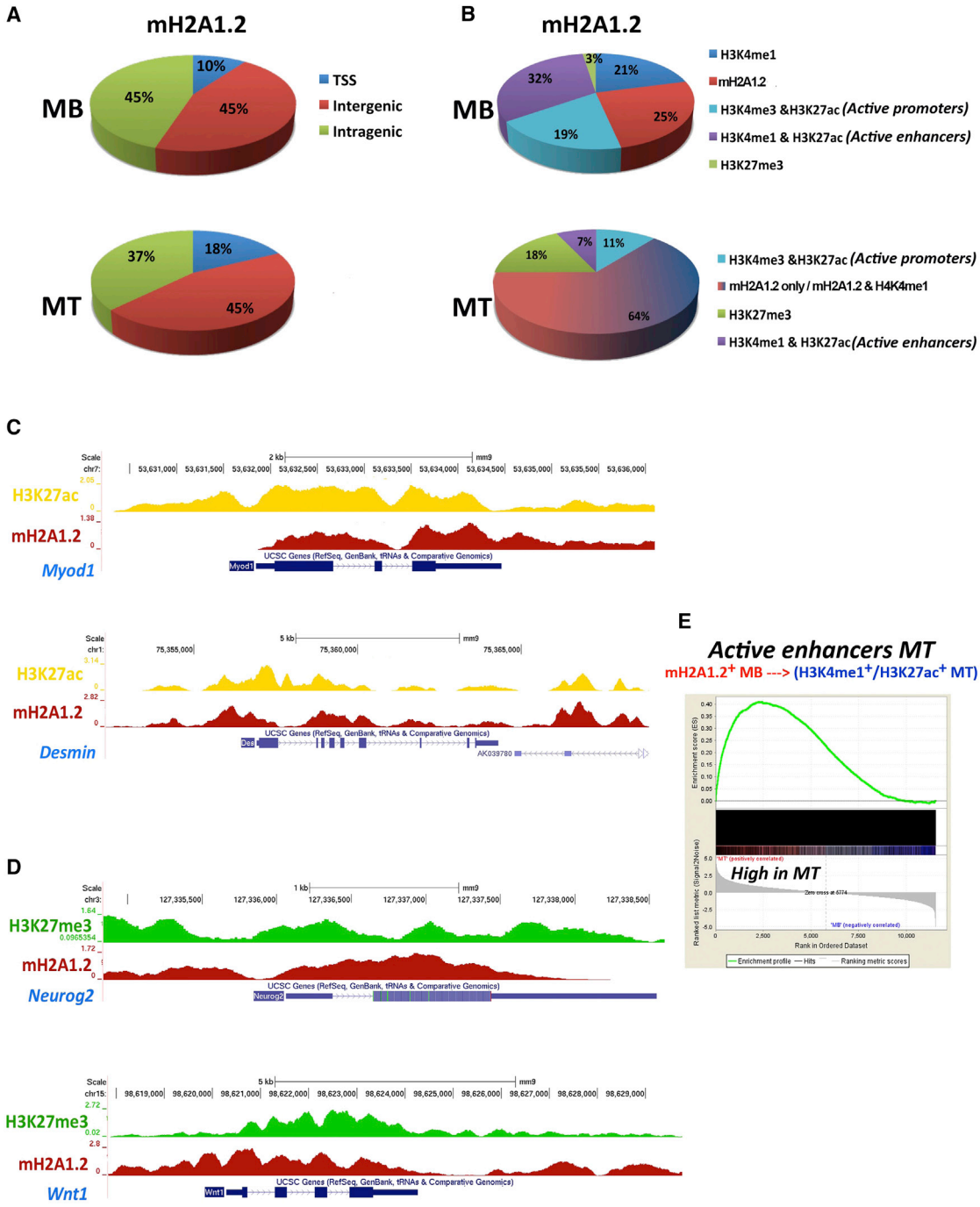

Figure 1. Genome-wide Distribution of the Histone Variant MacroH2A1.2 and Associated Epigenetic Marks at Regulatory Regions of Skeletal Muscle Cells

(A) Genome-wide distribution of mH2A1.2 in C2C12 MBs and MTs.

(B) Co-localization of mH2A1.2 and epigenetic marks H3K4me3, H3K4me1, H3K27ac, and H3K27me3 in C2C12 MBs and MTs.

(C) ChIP-seq profiles of mH2A1.2 and H3K27ac at *Myod1* and *Desmin* loci.

(D) ChIP-seq profiles of mH2A1.2 and H3K27me3 at *Neurogenin2* and *Wnt1* loci. Both H3K27ac and mH2A1.2 signals were corrected for input DNA.

(E) GSEA of genes assigned to MT-active enhancers bound by mH2A1.2 in MBs. Genes are ranked from left to right according to their Signal2Noise metric in MTs. The ES profile indicates that the gene set is enriched for upregulated genes in MT ($p < 2.0e\text{-}4$, false discovery rate [FDR] ~0).

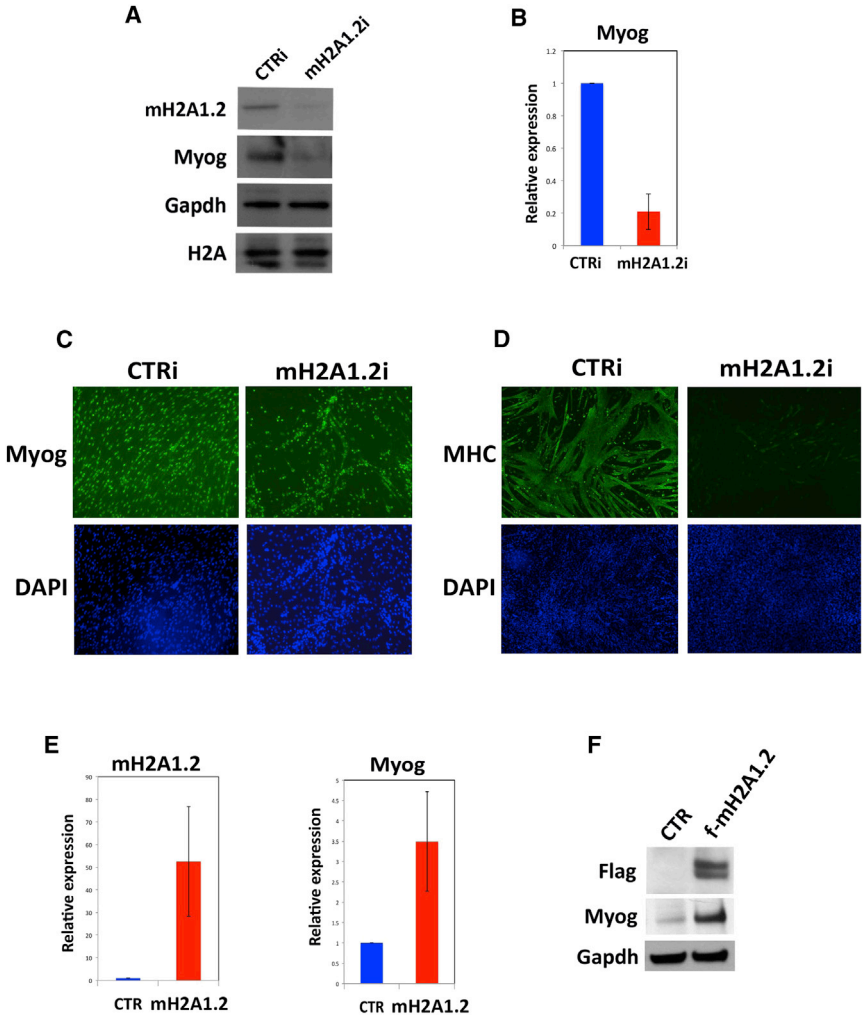

Figure 2. Reducing MacroH2A1.2 Impairs Skeletal Muscle Cell Differentiation

(A and B) Myogenin protein and mRNA evaluated after siRNA against mH2A1.2 in C2C12 cells. GAPDH and histone H2A were used as loading controls. CTRi, control.

(C and D) Myogenin (C) and MHC (D) immunofluorescence staining of control and mH2A1.2i C2C12 cells prompted to differentiate for 2 days. DAPI identifies nuclei.

(E) mH2A1.2 and Myogenin mRNA expression in C2C12 cells transfected with FLAG-empty (CTR) or FLAG-mH2A1.2 (f-mH2A1.2) expression vector (0.8 μg mH2A1.2 plasmid/1 × 10^5 cells).

(F) Immunoblot for FLAG, Myogenin, and GAPDH in C2C12 cells transfected with FLAG-empty (CTR) or FLAG-mH2A1.2 vector.

Data are represented as mean ± SD.

To define the global impact of reducing mH2A1.2 on the transcriptome, RNA-seq experiments were performed in control and mH2A1.2i C2C12 cells. When mH2A1.2i C2C12 MBs were induced to differentiate, a profound effect on transcriptional dynamics was observed. As indicated in the scatterplot representing changes in gene expression (Figure 3A), genes physiologically upregulated during cell differentiation failed to be properly activated in mH2A1.2i cells, while genes downregulated during differentiation remained transcribed. In control cells, expression of 2,392 genes was increased during the transition from MBs to MTs (Figure 3B; Table S3). Compared to control MTs, 1,786 gene transcripts were reduced by mH2A1.2i. Out of these 1,786 transcripts, 1,440 (80.5%) corresponded to transcripts increased during the differentiation of MBs to MTs (Figure 3B). GO analysis of the transcripts that failed to be appropriately upregulated in mH2A1.2i cells returned terms related to "muscle cell development" and "muscle cell differentiation" (Figure 3C). GO terms for the transcripts that remained elevated in mH2A1.2i cells were related to "cell cycle," "and "DNA replication" (Figure 3D). Myogenin and its downstream targets muscle creatine kinase (*Ckm*) and troponin T type 2 (*Tnnt2*) were not properly activated in mH2A1.2i cells (Figure 3E). Conversely, transcripts of the Inhibitor of DNA Binding 3 (*Id3*), a member of the Id family of helix-loop-helix proteins counteracting muscle differentiation (Benezra et al., 1990), cyclin D1 (*Ccnd1*), and the cell-cycle regulator *Mcm5*, which are physiologically downregulated upon C2C12 differentiation, remained abnormally elevated in mH2A1i cells (Figure 3F). To validate these findings, we used a different mH2A1.2 siRNA (mH2A1.2i_1) (Figure S3A). In mH2A1.2i_1-transfected cells, transcripts of Myogenin, muscle-specific MHC 3 (Myh3), cardiac actin (Actc1), and creatine kinase (Ckm) were reduced, while those of cyclin D (Ccnd1) remained elevated (Figure 3G). These findings indicate that mH2A1.2 is required to activate muscle gene expression during cell differentiation.

MacroH2A1.2 Is Enriched at Prospective Enhancers and Is Necessary for Their Activation

We used the assay for transposase-accessible chromatin with high-throughput sequencing (ATAC-seq) (Buenrostro et al., 2013) to define chromatin accessibility in C2C12 MBs and MTs. In ATAC-seq, tagging of nucleosome-free genomic regions is mediated by transposase-mediated delivery of sequencing adapters. Tagged regions correlate with DNase I hypersentitive sites (open chromatin), which are generally found within genomic regulatory functions. Using two independent replicates, ~47,300 and ~17,200 transposase-accessible or open chromatin regions were reproducibly identified in MBs and MTs, respectively (Figure 4A). More than 84% of these genomic regions (14,448/17,200) were open in both MBs and MTs (Figure 4B). The remaining ATAC-seq MT sites (~2,650) were closed in MBs and open in MTs, and almost all of them (~2,500) were located outside the promoter regions (Figures 4A and 4B). We refer to these two groups as constitutive (open in both MBs and MTs) and

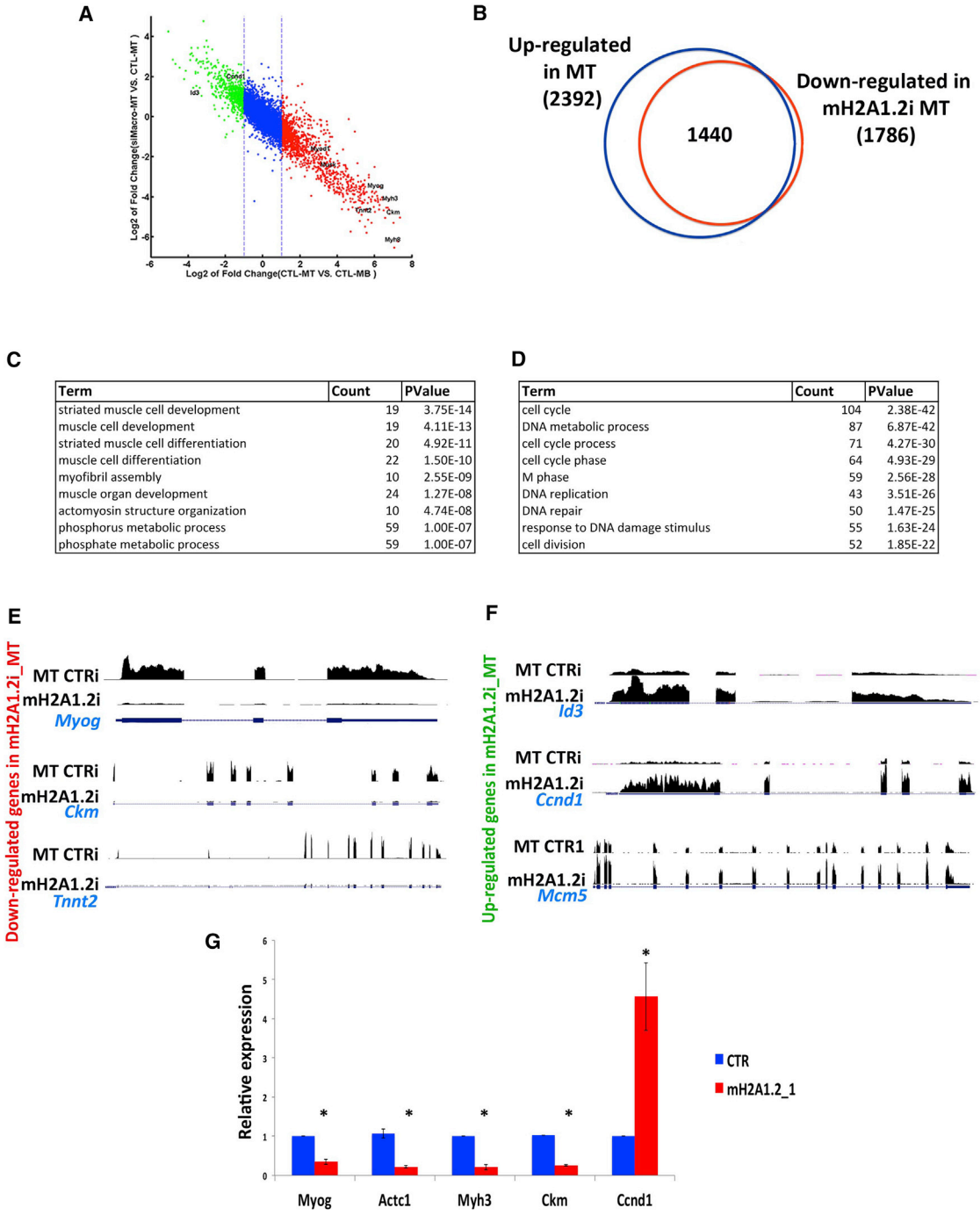

C

Term	Count	PValue
striated muscle cell development	19	3.75E-14
muscle cell development	19	4.11E-13
striated muscle cell differentiation	20	4.92E-11
muscle cell differentiation	22	1.50E-10
myofibril assembly	10	2.55E-09
muscle organ development	24	1.27E-08
actomyosin structure organization	10	4.74E-08
phosphorus metabolic process	59	1.00E-07
phosphate metabolic process	59	1.00E-07

D

Term	Count	PValue
cell cycle	104	2.38E-42
DNA metabolic process	87	6.87E-42
cell cycle process	71	4.27E-30
cell cycle phase	64	4.93E-29
M phase	59	2.56E-28
DNA replication	43	3.51E-26
DNA repair	50	1.47E-25
response to DNA damage stimulus	55	1.63E-24
cell division	52	1.85E-22

Figure 3. MacroH2A1.2 Regulates the Transcriptome of Differentiating Skeletal Muscle Cells

(A) Scatterplot shows the inhibitory effect of mH2A1.2 knockdown on transcriptome during differentiation. Each dot represents a gene, the x axis shows expression changes during differentiation in FLAG-empty vector (control; CTR), and the y axis shows the expression changes in mH2A1.2i versus CTR in MTs. Genes marked red and green are upregulated and downregulated during differentiation, respectively.

(B) Venn diagram illustrating number of genes upregulated in control C2C12 MT and downregulated in counterpart mH2A1.2i cells.

(C) GO for genes downregulated in differentiating mH2A1.2i C2C12 cells.

(D) GO for genes whose transcription remains elevated in differentiating mH2A1.2i C2C12 cells.

(E) RNA-seq profiles of downregulated genes *Myog*, *Ckm*, and *Tnnt2* in differentiating control interference (CTRi) and mH2A1.2i C2C12 cells.

(F) RNA-seq profiles of upregulated genes *Id3*, *Ccnd1*, and *Mcm5* in differentiating CTLi and mH2A1.2i C2C12 cells.

(G) Myogenin, Actc1, Myh3, Ckm, and Ccnd1 mRNAs were evaluated after siRNA against mH2A1.2 in C2C12 cells.

Data are represented as mean ± SD. *p < 0.01.

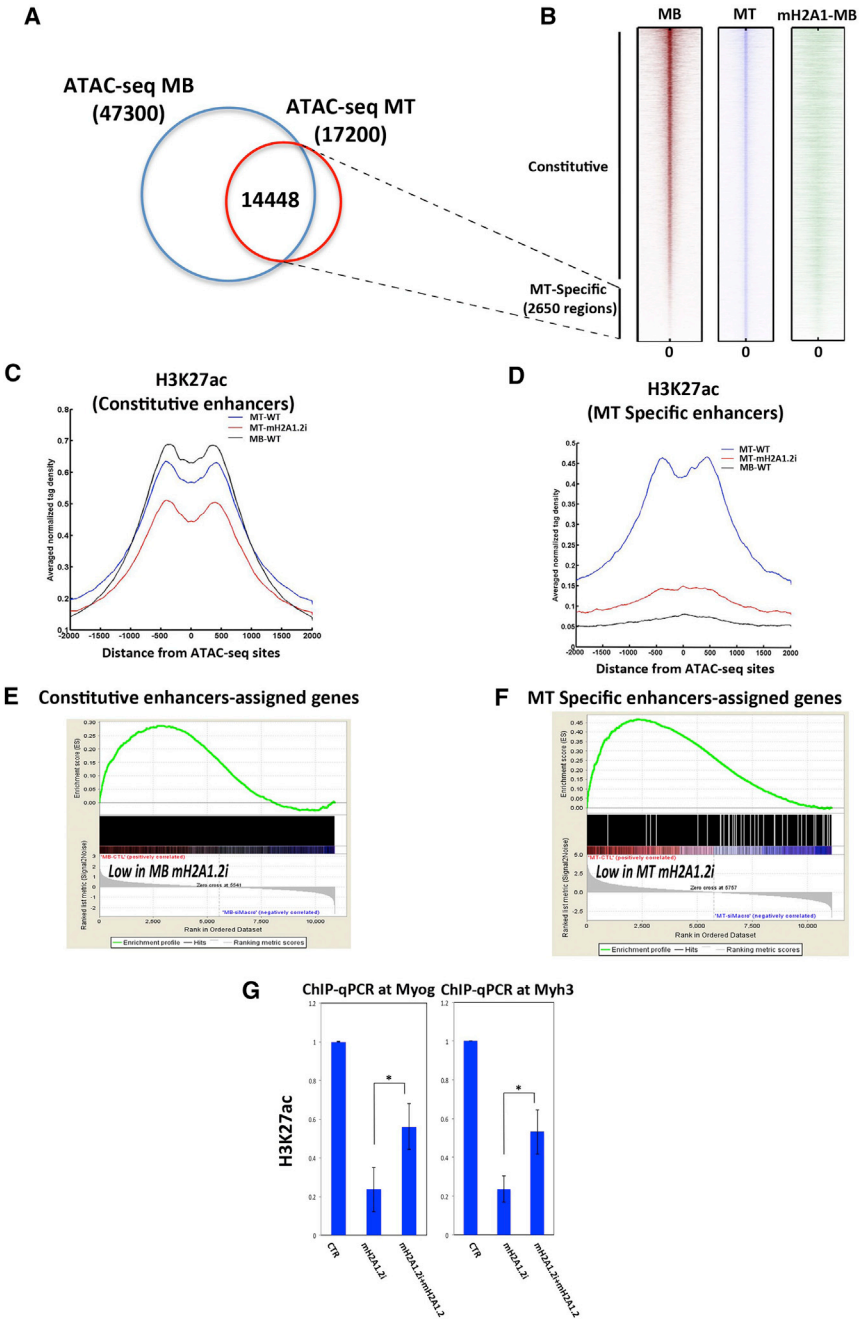

Figure 4. MacroH2A1.2 Influences H3K27 Acetylation at Enhancer Regions

(A) Venn diagram representing ATAC-seq positive regions in C2C12 MBs and MTs.

(B) Heatmaps of tag densities representing distribution of ATAC-seq signals in C2C12 MBs (red), MTs (blue), and mH2A1.2 binding (green) in MBs.

(C) Average profile of H3K27ac signal in C2C12 MBs (black line), MTs (blue line), and MT-mH2A1.2i (red line) for constitutive enhancers. WT, wild-type.

(D) Average profile of H3K27ac signal in MBs (black line), MTs (blue line) and MT-mH2A1.2i (red line) for MT-specific enhancers.

(E) GSEA of genes assigned to constitutive enhancers. Genes are ranked from left to right according to their Signal2Noise metric in MB-control (MB-CTR) versus MB-mH2A1.2i. The ES profile indicates that the gene set is enriched for downregulated genes in mH2A1.2i-MB ($p < 2.0e\text{-}4$, FDR < 10%).

(F) GSEA of genes assigned to MT-specific enhancers. Genes are ranked from left to right according to their Signal2Noise metric in MT-control (MT-CTR) versus MT-mH2A1.2i. The ES profile indicates that the gene set is enriched for genes strongly downregulated in mH2A1.2i-MT ($p < 2.0e\text{-}4$, FDR < 10%).

(G) ChIP-qPCR for H3K27ac at the *Myogenin* and *Myh3* loci in control (CTR), mH2A1.2i, and mH2A1.2i C2C12 cells transfected with mH2A1.2 expression vector.

Data are represented as mean ± SD. *$p < 0.01$.

MT-specific enhancers (present only in MTs), respectively. mH2A1.2 occupied both enhancer groups in MBs (Figure 4B). While constitutive enhancers were similarly acetylated at H3K27 in both MBs and MTs (Figure 4C; compare MB-WT, black line, and MT-WT, blue line), MT-specific enhancers acquired H3K27ac only in MTs (Figure 4D; compare MB-WT, black line, and MT-WT, blue line). To determine whether mH2A1.2 regulates the activity of constitutive and MT-specific enhancers, we assigned genes to these two groups of enhancers (based on proximity distance ±20 kb) and evaluated how mH2A1.2i affected expression of the enhancer-assigned genes. Using gene set enrichment analysis (GSEA), we found that genes assigned to constitutive enhancers were positively correlated with genes whose expression was reduced by mH2A1.2i in MBs (Figure 4E), whereas genes whose expression was diminished by mH2A1.2i in MTs correlated with genes assigned to MT-specific enhancers (Figure 4F). Since H3K27 acetylation is a defining step associated with enhancer activation (Creyghton et al., 2010; Heintzman et al., 2009; Rada-Iglesias et al., 2011; Zentner et al., 2011; Bonn et al., 2012), we evaluated whether mH2A1.2 was involved in conferring H3K27 acetylation by performing H3K27ac ChIP-seq on mH2A1.2i. H3K27 acetylation at constitutive enhancers was slightly reduced (Figure 4C; compare MT-WT, blue line, with MT-mH2A1.2i, red line). A most profound effect of mH2A1.2i on H3K27 acetylation was observed at MT-specific enhancers. At these enhancers, mH2A1i.2 reduced H3K27ac to background levels observed in MBs, where the chromatin of MT-specific enhancers is closed (Figure 4D; compare MT-WT, blue line, with MT-mH2A1.2i, red line). Consistent with a more limited reduction of H3K27ac at constitutive enhancers (Figure 4C), the transcription of genes assigned to constitutive enhancers was less affected than that of genes controlled by MT-specific enhancers

(Figure 4E; enrichment score [ES] < 0.30; Figure 4F, ES > 0.45) in mH2A1.2i cells. Next, we analyzed H3K27ac at promoter regions. mH2A1.2i did not modify H3K27ac at constitutive promoters but reduced it at MT-specific promoters (Figures S4A and S4B). These findings are consistent with the impaired acquisition of MT-specific enhancer competency upon mH2A1.2i and consequent failure to induce promoter activation (H3K27ac) and gene transcription. To establish whether a direct link exists between reduced H3K27 acetylation and mH2A1.2i, we attempted rescue experiments by overexpressing mH2A1.2 in mH2A1.2i cells. mH2A1.2 overexpression partially restored H3K27ac at both the Myogenin and Myh3 loci in mH2A1.2i cells (Figure 4G). In summary, these results indicate that, during muscle cell differentiation, mH2A1.2 is involved in conferring enhancer activation by regulating H3K27 acetylation.

Chromatin Engagement of the Transcription Factor Pbx1 at Muscle Regulatory Regions Is Contingent on MacroH2A1.2

The presence of mH2A1.2 in MBs at both TSSs and enhancers destined to become activated in MTs (MT-specific enhancers), as well as its requirement for their activation, prompted us to investigate a potential link between mH2A1.2 and the transcription factor Pbx1. The TALE (three-amino-acid loop extension) homeodomain-containing transcription factor Pbx1 is required to assist MyoD-dependent activation of *Myogenin* (Berkes et al., 2004; de la Serna et al., 2005). Pbx1 is constitutively bound to the *Myogenin* gene in fibroblasts prior to MyoD-mediated conversion to muscle and, by directly interacting with two specific domains, ensures productive and stable MyoD recruitment at the *Myogenin* promoter (Berkes et al., 2004). More recently, the Pbx1/MyoD interaction has been shown to regulate expression of a large cohort of MyoD-dependent genes (Fong et al., 2015). Suggesting a relationship between mH2A1.2 and Pbx1, analysis for DNA-binding motifs showed that, among others, the Pbx1 consensus binding motif was enriched within mH2A1.2-bound regions in MBs (Figure S5A). We performed Pbx1 ChIP-seq and examined the overlap between Pbx1 and MyoD binding (Mousavi et al., 2013). The majority of Pbx1 peaks occurred at inter-and intragenic regions in both MBs (88%) and MTs (76%) (Figures 5A and 5B). Approximately 57% of the Pbx1 peaks overlapped with MyoD in MB and 33% in MT, respectively (Figures 5C and 5D). Moreover, in MT, MyoD and Pbx1 co-occupied 52% of the MT-specific ATAC-seq regions (Figure 5E). Examples of muscle genes co-occupied by MyoD and Pbx1 are shown in Figure 5F. In line with the aforementioned observations, the E-box (DNA recognition site for MyoD) emerged as one of the top enriched motifs within Pbx1-occupied regions (Figures S5B and S5C). Similarly, de novo motif analysis of common binding regions between MBs and MTs returned, among others, motifs with consensus matching MyoD/Myf5 and Pbx3 (Figure S5D). In MB, 5,902 Pbx1 peaks occurred at genomic regions acquiring epigenetic characteristics of active enhancers ($H3K4me1^+$/$H3K27ac^+$) in MTs (Table S4). Of the genes assigned to MT-specific enhancers, 70% was also assigned to these $Pbx1^+$ regulatory regions (Table S4). To investigate a potential dependency of Pbx1 binding on mH2A1.2, we conducted Pbx1 ChIP-seq in control and mH2A1.2i cells. While overall Pbx1 binding was not affected at constitutive enhancers (Figure 6A), it was markedly decreased at MT-specific enhancers, including the *Myogenin* locus (Figures 6B–6D). Moreover, the promoters and/or enhancer regions of genes regulated by Pbx1 (Berkes et al., 2004) were co-occupied by Pbx1 and MyoD, and their transcription was reduced by mH2A1.2i (Figure 6E). Next, we evaluated whether mH2A1.2 is sufficient to promote Pbx1 recruitment by expressing FLAG-tagged mH2A1.2 and performing ChIP-qPCR for Pbx1 at *Myogenin*. Compared to control, Pbx1 recruitment at the *Myogenin* locus was increased in C2C12 mH2A1.2-transfected cells (Figure 6F). Importantly, Pbx1 transcripts were not affected by mH2A1.2 expression (Figure S6A). Thus, mH2A1.2 overexpression promotes Pbx1 engagement at *Myogenin* and activates its transcription (Figures 2E and 2F). Consistent with these findings, mH2A1.2 expression in mH2A1.2i cells partially restored Pbx1 binding at *Myogenin* (Figure 6G). In line with a role of Pbx1 in stabilizing MyoD binding (Berkes et al., 2004), MyoD engagement at *Myogenin* was also reduced by mH2A1.2i (Figure 6H). Overexpressed as well as endogenous and chromatin-bound mH2A1.2 interacted with Pbx1 (Figures S6B and S6C) and, using bacterially produced and purified proteins, we detected an interaction of the macro domain—but not of the H2A-like region—of mH2A1.2 with Pbx1 (Figure S6D). Pbx1 also interacted with canonical H2A (data not shown). Altogether, the data reported in this paragraph indicate that mH2A1.2 regulates Pbx1 recruitment at developmental (MT-specific) enhancers and transcription of the associated genes.

DISCUSSION

Here, we report that mH2A1.2 is a positive regulator of transcription and muscle cell differentiation. In agreement with previous studies, we have identified genomic regions co-occupied by mH2A1.2 and H3K27me3 (Buschbeck et al., 2009; Ratnakumar et al., 2012; Gaspar-Maia et al., 2013). However, mH2A1.2 knockdown neither modified H3K27me3 (data not shown) nor resulted in gene de-repression (Table S3), suggesting that, similary to what was observed with pluripotency genes (Gaspar-Maia et al., 2013), mH2A1.2 may play a redundant silencing role. Genome-wide distribution of mH2A1.2 localized at transcriptionally competent regulatory regions in undifferentiated C2C12 MBs. However, competency of constitutive enhancers was only modestly affected by mH2A1.2i, indicating that, once enhancers are activated, mH2A1.2 may not be critical for their maintenance. Instead, mH2A1.2 exerted a critical function during the differentiation process. Reducing mH2A1.2 prevented activation of the myogenic gene regulatory network, with approximately 80% of the genes whose transcription is promoted during differentiation failing to be activated. This phenomenon coincided with the inability of muscle developmental enhancers to be appropriately H3K27 acetylated in mH2A1.2i cells.

The presence of mH2A1.2 at prospective enhancers and its requirement for their activation suggest that mH2A1.2 functions as a "marking" histone (Bell et al., 2011). Pioneer transcription factors can access silent chromatin by recognizing their complete or partial DNA motifs on nucleosomes followed by the subsequent binding of other transcription factors and chromatin

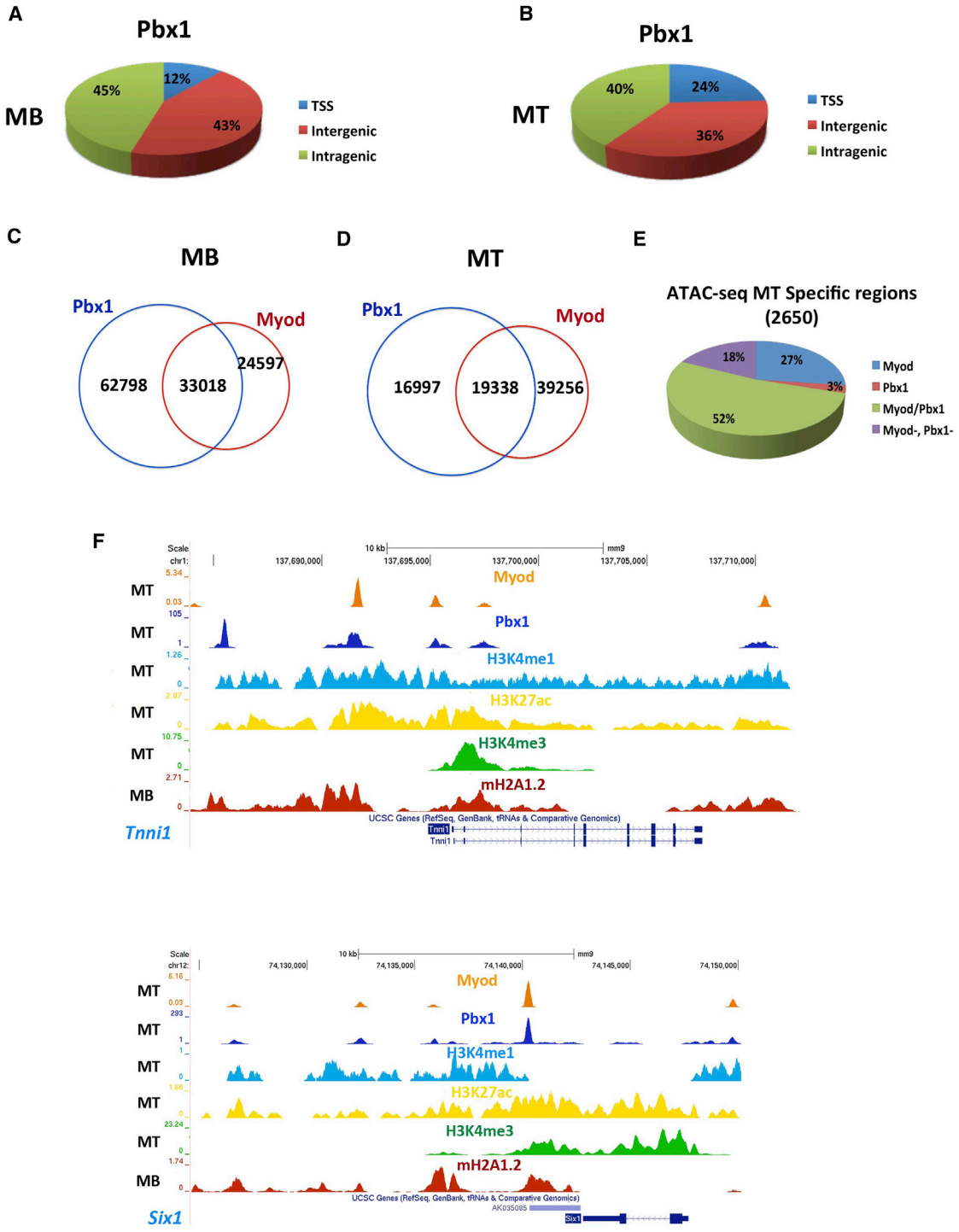

Figure 5. Genome-wide Analysis of Pbx1 and MyoD Binding in Skeletal Muscle Cells

(A and B) Genome-wide distribution of Pbx1 binding in C2C12 MBs and MTs.

(C and D) Venn diagrams representing Pbx1 and MyoD peaks in C2C12 MBs and MTs.

(E) MyoD and Pbx1 distribution relative to MT-specific ATAC-seq regions.

(F) ChIP-seq tracks at the *Tnnt1* and *Myh3* loci. Bottom to top: mH2A1.2 in MBs (red track), H3K4me3 in MTs (green track), H3K27ac in MTs (yellow track), H3K4me1 in MTs (blue track), Pbx1 in MTs (blue tracks), and MyoD in MTs (orange track). The ChIP-seq signals were corrected for input DNA.

remodelers (Zaret and Carroll, 2011; Iwafuchi-Doi and Zaret, 2014; Soufi et al., 2015). MyoD can convert non-myogenic cells to adopt the skeletal muscle phenotype (Davis et al., 1987). The ability of MyoD to initiate myogenesis in non-muscle cells is conferred by two independent domains, the cysteine-rich domain and the C-terminal helix III region (Gerber et al., 1997; Bergstrom and Tapscott, 2001). These two domains ensure stable binding of MyoD to the *Myogenin* promoter via interaction with a protein complex containing Pbx1, a homeodomain transcription factor constitutively bound to the *Myogenin* promoter (Berkes et al., 2004; de la Serna et al., 2005). Pbx1 has been proposed to act as a pioneer factor to guide chromatin recruitment of estrogen receptors in breast cancer (Magnani et al., 2011). Our findings indicate that mH2A1.2 exerts a licensing function for Pbx1 recruitment and H3K27 acetylation. The observed anti-correlation between mH2A1.2 occupancy and Pbx1 binding at MT-specific enhancers in MTs (Figure 6B; Figure S2B) suggests that, once enhancers are bound by Pbx1 (and/or MyoD), the mH2A1.2-containing nucleosomes are disassembled and mH2A1.2 may dissociate from its target regions during chromatin remodeling events. It has been recently shown that pioneer activity can be achieved by different strategies. While the prototypic pioneer factor FoxA exploits the homology of its DNA-binding domain with linker histone to interact with its DNA motif exposed on nucleosomes (Clark et al., 1993; Ramakrishnan et al., 1993; Cirillo and Zaret, 1999; Cirillo et al., 2002), the reprogramming factor Oct4 can target partial sequences of its DNA-binding motif, using the two separate PouS and PouHD domains, and Sox2 may take advantage of the pre-bent conformation of its DNA-binding motif, as well as its nonspecific DNA binding properties (Soufi et al., 2015). To penetrate and remodel closed chromatin, MyoD requires the two regions that interact with Pbx (Gerber et al., 1997; Bergstrom and Tapscott, 2001; Berkes et al., 2004), and point mutations abolishing Pbx interaction redirect MyoD binding toward neuronal targets (Fong et al., 2015). Decreased Pbx1 recruitment at *Myogenin* after mH2A1.2 knockdown was partially rescued by mH2A1.2 overexpression. While the most parsimonious explanation of this phenomenon is that mH2A1.2 favors Pbx1 chromatin engagement, we cannot formally rule out that unidentified factor/s may directly or indirectly be involved. Our data suggest the possibility that, by interacting with the macro domain of mH2A1.2, Pbx1 may gain access to repressed chromatin. However, canonical H2A also interacted with Pbx1. Despite the high homology between canonical H2A and the H2A-like domain of mH2A1.2 (Chakravarthy et al., 2005), the latter does not interact with Pbx1, indicating specificity of Pbx1 interaction within the mH2A1.2 moiety. As mH2A1.2 tends to form hybrid nucleosomes containing canonical H2A and H2B (Chakravarthy and Luger, 2006), Pbx1-binding specificity may arise from unique H2A-H2B-mH2A1.2 combinatorial composition of the nucleosomes. The mH2A1 macro domain interacts with histone deacetylases (Chakravarthy et al., 2005), and mH2A1 phosphorylation at serine 137 results in its exclusion from the heterochromatin of the inactive X chromosome (Bernstein et al., 2008). It is, therefore, possible that post-translational modifications may participate in imparting alternative functions to mH2A1 by modulating protein-protein interactions.

EXPERIMENTAL PROCEDURES

Cell Culture and Reagents

All cells were cultured at 37°C with 5% CO_2. Cell media were supplemented with 500 μg/ml penicillin-streptomycin-glutamine (GIBCO). Both HEK293 and C2C12 cells (ATCC) were grown in 1× DMEM with 10% qualified fetal bovine serum (FBS) (GIBCO). For C2C12 cell differentiation, FBS was replaced with 2% horse serum and 1× insulin-transferrin-selenium (GIBCO). For siRNA experiments, cells were transfected with Lipofectamine RNAiMax (Invitrogen) according to the manufacturer's instructions. siRNA sequences are reported in Table S5. Plasmids were transfected in C2C12 cells using Lipofectamine 2000 (Invitrogen).

Antibodies

A list of the antibodies used is reported in the Supplemental Experimental Procedures.

Plasmid Construction

Plasmid construction is reported in the Supplemental Experimental Procedures.

Protein Expression and Purification

GST fusion proteins were expressed in *E. coli* and purified using Glutathione Sepharose 4B (GE Healthcare Life Sciences) according to manufacturer's protocol. His-Pbx1a was expressed in *E. coli* and purified using HisPur Cobalt Resin (Thermo Scientific) according to manufacturer's protocol.

In Vitro Protein Interaction

Purified His-Pbx1a and glutathione S-transferase (GST)-macroH2A1.2 proteins were incubated with anti-Pbx1 antibody (Abnova, H00005087) in immunoprecipitation (IP) buffer (20 mM Tris-HCl [pH 8.0], 10% glycerol, 0.15 M KCl, 5 mM $MgCl_2$, 0.1% NP-40), and the complexes bound to protein A agarose (Roche) were washed three times with IP buffer (with 0.5 M KCl) and once with IP buffer (with 0.15 M KCl). The interaction between Pbx1-a and GST proteins was detected by western blot with anti-Pbx1 and anti-GST (Santa Cruz Biotechnology, sc-459) antibodies.

IPs

For co-IP, HEK293T cells were co-transfected with plasmids expressing Pbx1a (Addgene, #21029) and FLAG-tagged macroH2A1.2 and harvested with lysis buffer (20 mM Tris-HCl [pH 8.0], 10% glycerol, 150 mM NaCl, 5 mM $MgCl_2$, 0.1% NP-40, protease inhibitor cocktail). 1 mg whole-cell lysate was incubated with anti-FLAG M2-agarose beads (Sigma). Protein interactions were detected by western blot with anti-Pbx1 (Abnova H00005087) and anti-FLAG (M2, Sigma) antibodies.

Chromatin Fraction Isolation and IP

Detailed protocols for chromatin isolation and IP are reported in the Supplemental Experimental Procedures.

ChIP-qPCR and ChIP-Seq

Cells were crosslinked in 1% formaldehyde and processed according to published protocols (Métivier et al., 2003; Mousavi et al., 2012). Briefly, cells were lysed in RIPA buffer (1× PBS, 1% NP-40, 0.5% sodium deoxycholate, 0.1% SDS) and centrifuged at 2,000 rpm for 5 min. The chromatin fraction was sheared by sonication (four times, each lasting 30 s) in 1.5-ml siliconized Eppendorf tubes. The resulting sheared chromatin samples were cleared for 1 hr, immunoprecipitated overnight, and washed in buffer I (20 mM Tris-HCl [pH 8.0], 150 mM NaCl, 2 mM EDTA, 0.1% SDS, 1% Triton X-100), buffer II (20 mM Tris-HCl [pH 8.0], 500 mM NaCl, 2 mM EDTA, 0.1% SDS, 1% Triton X-100), buffer III (10 mM Tris-HCl [pH 8.0] 250 mM LiCl, 1% NP-40; 1% sodium deoxycholate, 1 mM EDTA), and Tris-EDTA (pH 8.0). All washes were performed at 4°C for 5 min. Finally, crosslinking was reversed in elution buffer (100 mM $NaHCO_3$, 1% SDS) at 65°C overnight. Real-time qPCR was performed using Power SYBR Green PCR Master Mix (Applied Biosystems) following the standard procedure. A list of primers used for qPCR is provided in Table S5. For ChIP-seq, 10 ng immuno-precipitated DNA fragments were

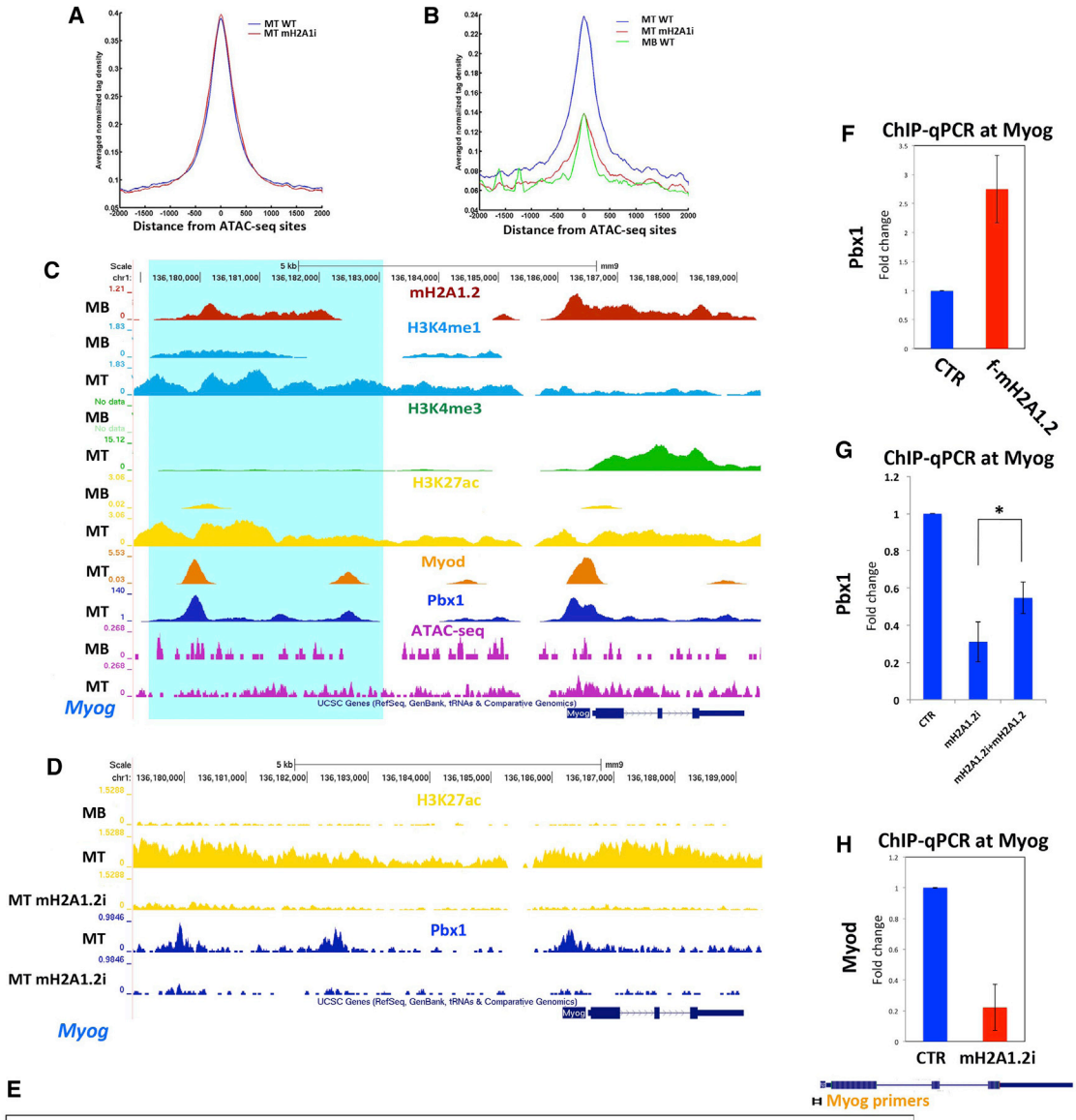

E

Pbx1- dependent genes

Genes			Pbx1+ MB		Myod+ MB		Pbx1+ MT		Myod+ MT				Active enhancers-assigned genes_ MT
GenBank	UniGene	Gene Symbol	Prom	Enhancers	Prom	Enhancer	Prom	Enhancers	Prom	Enhancer	UP from MB to MT	Down_MT mH2A1i	mH2A1+_MB/ H3K4me1+/H3K27ac+_MT
X15784	Mm.16528	Myog		YES	YES	YES	YES	YES	YES	YES	YES	YES	YES
AJ242874	Mm.36900	Tnni (Tnni1)		YES		YES		YES	YES	YES	YES	YES	YES
AI427516	Mm.14802	H19					YES		YES		YES	YES	YES
NM_009394	Mm.1716	Tncs (Tnnc2)		YES				YES		YES	YES	YES	YES
NM_016754	Mm.14526	Mylpf		YES				YES	YES	YES	YES	YES	YES
AI385643	Mm.200230	Mybph		YES		YES	YES	YES	YES	YES	YES	YES	NO
AI451106	Mm.103675	Sacs	YES	YES	YES	YES	YES	YES	YES	YES	YES	YES	YES
M38129	Mm.2780	Myh3	YES				YES	YES	YES	YES	YES	YES	YES
NM_008506	Mm.1055	Lmyc1		YES		YES	YES	YES	YES	YES	YES	YES	NO
M74541	Mm.1976	Cdh15	YES	YES	YES	YES	YES	YES	YES	YES	YES	YES	YES
X83932	Mm.233726	Ryr1	YES	YES	YES	YES	YES	YES			YES	YES	YES
AI450282	Mm.4913	Fst		YES		YES		YES		YES	YES	YES	YES
X80339	Mm.4645	Six1	YES	YES			YES	YES		YES	NO	NO	NO
AI428883	Mm.26835	Spint2						YES		YES	NO	NO	NO
AI428484	Mm.30841	Cacna2d1	YES	YES		YES	YES	YES		YES	YES	YES	NO

Figure 6. MacroH2A1.2 Regulates Recruitment of Pbx1 at Muscle Enhancer Regions

(A) Average profile of Pbx1 signal in MT-WT (blue line) and differentiating mH2A1.2i C2C12 cells (red line) at constitutive enhancers.

(B) Average profiles of Pbx1 signal in MT-WT (blue line), in MT-mH2A1.2i (red line), and in MB-WT at MT-specific enhancers.

(C) ChIP-seq tracks at the *Myogenin* locus. Top to bottom: mH2A1.2 in MTs and MBs (red tracks); H3K4me1 in MBs and MTs (light blue tracks); H3K4me3 in MBs and MTs (green tracks); H3K27ac in MBs and MTs (yellow tracks); MyoD in MTs (orange track); Pbx1 in MTs (blue tracks); and ATACseq signal in MBs and sMT (purple tracks). Turquoise shading identifies an H3K27ac^{+}/H3K4me1^{+}/Pbx1^{+}/MyoD^{+}/H3K4me3^{-} region.

(D) ChIP-seq tracks at the *Myogenin* locus. Top to bottom: H3K27ac in MBs, MTs, and MT_mH2A1.2i (yellow tracks); Pbx1 in MT-control (MT-CTR) and mH2A1.2i (blue tracks).

(legend continued on next page)

used to prepare ChIP-seq libraries with the NEBNext RNA Library Prep Kit (New England Biolabs) and the Ovation SP Ultralow DR Multiplex System (NuGEN) following the manufacturer's protocol. The libraries were sequenced for 50 cycles on a HiSeq 2000 or HiSeq2500 Illumina instrument.

RNA-Seq

mRNA sequencing (mRNA-seq) (poly(A)$^+$ fraction) samples were prepared and processed according to the manufacturer's protocol (Illumina). Briefly, total RNA was extracted from approximately 1 × 10^6 C2C12 cells using the Trizol reagent. 500 ng of total RNA was retrotranscribed using the High Capacity cDNA Reverse Transcription Kit (Applied Biosystems). qPCR was performed with the Power SYBR Green PCR Master Mix (Applied Biosystems). All primers used for amplification are listed in Table S5. 1 μg to 3 μg of total RNA was used to prepare RNA-seq libraries with the NEBNext RNA Library Prep Kit (New England Biolabs) and the Ovation SP Ultralow DR Multiplex System (NuGEN), following the manufacturer's protocol. The libraries were sequenced for 50 cycles (single-end reads) on a HiSeq 2000 or HiSeq2500 Illumina instrument.

ATAC-Seq

ATAC-seq was performed according to a published protocol (Buenrostro et al., 2013), with minor modification. Briefly, 5 × 10^4 C2C12 cells were pelleted, washed with 50 μl of 1× PBS, and lysed in 50 μl lysis buffer (10 mM Tris-HCl,[pH 7.4], 10 mM NaCl, 3 mM $MgCl_2$, 0.1% IGEPAL CA-630). To tag and fragment accessible chromatin, nuclei were centrifuged at 500 × g for 10 min and re-suspended in 40 μl transposition reaction mix with 2 μl Tn5 transposase (Illumina #FC-121-1030). The reaction was incubated at 37°C, with shaking at 300 rpm for 30 min. DNA fragments were then purified and amplified by PCR (12–15 cycles based on the amplification curve). C2C12 MB and MT samples were multiplexed using primers Ad2.1–4 paired with Ad1 for final library amplification as described previously (Buenrostro et al., 2013). Purified libraries were then sequenced on a HiSeq2500 Illumina instrument.

Venn Diagrams

The area-proportional Venn diagrams were drawn based on images generated using free online software (http://bioinforx.com/free/bxarrays/venndiagram.php).

Bioinformatic Analysis

RNA-Seq Analysis

Whole-transcriptome sequencing (RNA-seq) of C2C12 MBs and MTs for control and mH2A1.2i in three biological replicates were completed on HiSeq2000/2500 Illumina instruments, using cDNA libraries generated from poly(A)$^+$ purified mRNA samples. 50-bp single-end reads were mapped to mouse genome (mm9 assembly) using TopHat (Trapnell et al., 2009), and gene transcript levels were determined via Cuffdiff in the form of fragments per kilobase of exon per million fragments mapped, or FPKM (RPKM [reads per kilobase of exon per million reads mapped]) values, by correcting for multi-reads and using geometric normalization (Trapnell et al., 2013). Up- and downregulated genes were selected using 1.5-fold change cutoff, and only genes with a mean RPKM value of >1 in at least one condition were included. GO analyses for a list of selected genes were performed by the online bioinformatics resource DAVID (National Institute of Allergy and Infectious Diseases, NIH) (Huang et al., 2009a, 2009b).

ChIP-Seq and ATAC-Seq Analyses

ChIP-seq data from two biological replicates for each sample were obtained using HiSeq 2000/2500 Illumina instruments, de-multiplexed through an Illumina pipeline, and mapped to the mouse genome (mm9 assembly) using the Bowtie algorithm (Langmead et al., 2009), with default parameters except for seed length set to 32 and suppressing all alignments for reads if more than 20 were presented. ChIP-seq data generated from genomic DNA (input DNA) or immunoglobulin G (IgG) were used as a control for calling enriched regions. Peaks for macroH2A1 and Pbx1 were called using MACS, version 2 (Zhang et al., 2008), with q value set at 0.05. Previously published ChIP-seq data for MyoD in MBs and MTs (Mousavi et al., 2013) were re-analyzed using similar parameters. Regions of open chromatin were identified using MACS from ATAC-seq data obtained from two biological replicates in C2C12 MBs and MTs. Only regions called in both replicates were used in downstream analysis. In all cases, redundant reads were removed, and only one mapped read to each unique regions of the genome was kept and used in peak calling. Peaks were assigned to promoters if they were located in the ±1,000-bp vicinity of TSS; assigned to intragenic if they were located in gene body, excluding +1,000 bp of TSS; and assigned to intergenic otherwise. For generating the profile of different marks across TSSs or ATAC-seq sites, aligned reads, after removing redundant reads, were directly mapped to sliding windows of 100 bp in 25-bp steps, at ±2,000 bp around the center of ATAC-seq peaks or ±5,000 bp around the TSS. Signals were averaged across all sites and normalized to the total number of reads for each sample. Profiles and HeatMap, as well as other downstream analyses, were done using custom programing in MATLAB. GSEA was done using GSEA tools (Subramanian et al., 2005; Mootha et al., 2003), with number of permutation set to 5,000, and permutation was applied to the gene set. Gene lists were generated by assigning genes to the genomic regions of interest (e.g., enhancers), using a proximity distance of ±20 kbp of gene body (region of interest lies within the interval of TSS− 20 kbp, TES [transcription end site]+ 20 kbp), increasing the proximity distance to ±50 kbp or ±100 kbp, while increasing the number of total and false-positive assigned genes did not returned any new enriched GO terms. The BEDTools package (Quinlan and Hall, 2010) was handy for several applications, including intersecting regions, generating BedGraph files converted to Bigwig files presented in genome browser tracks, filtering reads, etc. Motif enrichment and de novo motif analysis were carried out using the Homer package (Heinz et al., 2010) for regions spanning 200 bp around the peaks' summit.

ACCESSION NUMBERS

The accession number for the RNA-seq and ChIP-seq datasets reported in this paper is GEO: GSE76010.

SUPPLEMENTAL INFORMATION

Supplemental Information includes Supplemental Experimental Procedures, six figures, and five tables and can be found with this article online at http://dx.doi.org/10.1016/j.celrep.2015.12.103.

AUTHOR CONTRIBUTIONS

S.D., H.Z., and V.S. designed the experiments. S.D., A.H.W., H.-Y.S., and K.S. conducted the experiments and analyzed the data. H.Z. designed and conducted computational analysis. L.B. and A.G.L. contributed reagents. G.G.-C. supervised sequencing experiments. J.J.O. supervised H.-Y.S. and analyzed the data. S.D., H.Z., and V.S. wrote the manuscript, with input from the other authors.

ACKNOWLEDGMENTS

We thank members of the V.S. laboratory for helpful discussion and technical advice. This work was supported in part by the Intramural Research Program of NIAMS.

(E) Summary of Pbx1and MyoD occupancy in MBs and MTs, expression in MBs and MTs, expression in mH2A1.2i cells, and assignment to MT-specific enhancers of Pbx1-dependent genes reported in Berkes et al. (2004).
(F) Pbx1 ChIP-qPCR in CTR and mH2A1.2-overexpressing (2 μg mH2A1.2 plasmid/1 × 10^5 cells).
(G) ChIP-qPCR for Pbx1 at the *Myogenin* locus in control (CTR), mH2A1.2i, and mH2A1.2i C2C12 cells transfected with mH2A1.2 expression vector.
(H) ChIP-qPCR for MyoD at the *Myogenin* locus in control (CTR) and mH2A1.2i C2C12 cells.
Data are represented as mean ± SD. *$p < 0.01$.

Received: May 18, 2015
Revised: November 10, 2015
Accepted: December 23, 2015
Published: January 28, 2016

REFERENCES

Barrero, M.J., Sese, B., Kuebler, B., Bilic, J., Boue, S., Martí, M., and Izpisua Belmonte, J.C. (2013). Macrohistone variants preserve cell identity by preventing the gain of H3K4me2 during reprogramming to pluripotency. Cell Rep. *3*, 1005–1011.

Barski, A., Cuddapah, S., Cui, K., Roh, T.Y., Schones, D.E., Wang, Z., Wei, G., Chepelev, I., and Zhao, K. (2007). High-resolution profiling of histone methylations in the human genome. Cell *129*, 823–837.

Bell, O., Tiwari, V.K., Thomä, N.H., and Schübeler, D. (2011). Determinants and dynamics of genome accessibility. Nat. Rev. Genet. *12*, 554–564.

Benezra, R., Davis, R.L., Lockshon, D., Turner, D.L., and Weintraub, H. (1990). The protein Id: a negative regulator of helix-loop-helix DNA binding proteins. Cell *61*, 49–59.

Bergstrom, D.A., and Tapscott, S.J. (2001). Molecular distinction between specification and differentiation in the myogenic basic helix-loop-helix transcription factor family. Mol. Cell. Biol. *21*, 2404–2412.

Berkes, C.A., Bergstrom, D.A., Penn, B.H., Seaver, K.J., Knoepfler, P.S., and Tapscott, S.J. (2004). Pbx marks genes for activation by MyoD indicating a role for a homeodomain protein in establishing myogenic potential. Mol. Cell *14*, 465–477.

Bernstein, E., Muratore-Schroeder, T.L., Diaz, R.L., Chow, J.C., Changolkar, L.N., Shabanowitz, J., Heard, E., Pehrson, J.R., Hunt, D.F., and Allis, C.D. (2008). A phosphorylated subpopulation of the histone variant macroH2A1 is excluded from the inactive X chromosome and enriched during mitosis. Proc. Natl. Acad. Sci. USA *105*, 1533–1538.

Bonn, S., Zinzen, R.P., Girardot, C., Gustafson, E.H., Perez-Gonzalez, A., Delhomme, N., Ghavi-Helm, Y., Wilczyński, B., Riddell, A., and Furlong, E.E. (2012). Tissue-specific analysis of chromatin state identifies temporal signatures of enhancer activity during embryonic development. Nat. Genet. *44*, 148–156.

Buenrostro, J.D., Giresi, P.G., Zaba, L.C., Chang, H.Y., and Greenleaf, W.J. (2013). Transposition of native chromatin for fast and sensitive epigenomic profiling of open chromatin, DNA-binding proteins and nucleosome position. Nat. Methods *10*, 1213–1218.

Buschbeck, M., Uribesalgo, I., Wibowo, I., Rué, P., Martin, D., Gutierrez, A., Morey, L., Guigó, R., López-Schier, H., and Di Croce, L. (2009). The histone variant macroH2A is an epigenetic regulator of key developmental genes. Nat. Struct. Mol. Biol. *16*, 1074–1079.

Chakravarthy, S., and Luger, K. (2006). The histone variant macro-H2A preferentially forms "hybrid nucleosomes". J. Biol. Chem. *281*, 25522–25531.

Chakravarthy, S., Gundimella, S.K., Caron, C., Perche, P.Y., Pehrson, J.R., Khochbin, S., and Luger, K. (2005). Structural characterization of the histone variant macroH2A. Mol. Cell. Biol. *25*, 7616–7624.

Chen, H., Ruiz, P.D., Novikov, L., Casill, A.D., Park, J.W., and Gamble, M.J. (2014). MacroH2A1.1 and PARP-1 cooperate to regulate transcription by promoting CBP-mediated H2B acetylation. Nat. Struct. Mol. Biol. *21*, 981–989.

Cirillo, L.A., and Zaret, K.S. (1999). An early developmental transcription factor complex that is more stable on nucleosome core particles than on free DNA. Mol. Cell *4*, 961–969.

Cirillo, L.A., Lin, F.R., Cuesta, I., Friedman, D., Jarnik, M., and Zaret, K.S. (2002). Opening of compacted chromatin by early developmental transcription factors HNF3 (FoxA) and GATA-4. Mol. Cell *9*, 279–289.

Clark, K.L., Halay, E.D., Lai, E., and Burley, S.K. (1993). Co-crystal structure of the HNF-3/fork head DNA-recognition motif resembles histone H5. Nature *364*, 412–420.

Costanzi, C., and Pehrson, J.R. (1998). Histone macroH2A1 is concentrated in the inactive X chromosome of female mammals. Nature *393*, 599–601.

Costanzi, C., and Pehrson, J.R. (2001). MACROH2A2, a new member of the MARCOH2A core histone family. J. Biol. Chem. *276*, 21776–21784.

Creppe, C., Janich, P., Cantariño, N., Noguera, M., Valero, V., Musulén, E., Douet, J., Posavec, M., Martín-Caballero, J., Sumoy, L., et al. (2012). MacroH2A1 regulates the balance between self-renewal and differentiation commitment in embryonic and adult stem cells. Mol. Cell. Biol. *32*, 1442–1452.

Creyghton, M.P., Cheng, A.W., Welstead, G.G., Kooistra, T., Carey, B.W., Steine, E.J., Hanna, J., Lodato, M.A., Frampton, G.M., Sharp, P.A., et al. (2010). Histone H3K27ac separates active from poised enhancers and predicts developmental state. Proc. Natl. Acad. Sci. USA *107*, 21931–21936.

Csankovszki, G., Nagy, A., and Jaenisch, R. (2001). Synergism of Xist RNA, DNA methylation, and histone hypoacetylation in maintaining X chromosome inactivation. J. Cell Biol. *153*, 773–784.

Davis, R.L., Weintraub, H., and Lassar, A.B. (1987). Expression of a single transfected cDNA converts fibroblasts to myoblasts. Cell *51*, 987–1000.

de la Serna, I.L., Ohkawa, Y., Berkes, C.A., Bergstrom, D.A., Dacwag, C.S., Tapscott, S.J., and Imbalzano, A.N. (2005). MyoD targets chromatin remodeling complexes to the myogenin locus prior to forming a stable DNA-bound complex. Mol. Cell. Biol. *25*, 3997–4009.

Doyen, C.M., An, W., Angelov, D., Bondarenko, V., Mietton, F., Studitsky, V.M., Hamiche, A., Roeder, R.G., Bouvet, P., and Dimitrov, S. (2006). Mechanism of polymerase II transcription repression by the histone variant macroH2A. Mol. Cell. Biol. *26*, 1156–1164.

Feng, J., Liu, T., Qin, B., Zhang, Y., and Liu, X.S. (2012). Identifying ChIP-seq enrichment using MACS. Nat. Protoc. *7*, 1728–1740.

Fong, A.P., Yao, Z., Zhong, J.W., Johnson, N.M., Farr, G.H., 3rd, Maves, L., and Tapscott, S.J. (2015). Conversion of MyoD to a neurogenic factor: binding site specificity determines lineage. Cell Rep. *10*, 1937–1946.

Gamble, M.J., and Kraus, W.L. (2010). Multiple facets of the unique histone variant macroH2A: from genomics to cell biology. Cell Cycle *9*, 2568–2574.

Gamble, M.J., Frizzell, K.M., Yang, C., Krishnakumar, R., and Kraus, W.L. (2010). The histone variant macroH2A1 marks repressed autosomal chromatin, but protects a subset of its target genes from silencing. Genes Dev. *24*, 21–32.

Gaspar-Maia, A., Qadeer, Z.A., Hasson, D., Ratnakumar, K., Leu, N.A., Leroy, G., Liu, S., Costanzi, C., Valle-Garcia, D., Schaniel, C., et al. (2013). MacroH2A histone variants act as a barrier upon reprogramming towards pluripotency. Nat. Commun. *4*, 1565.

Gerber, A.N., Klesert, T.R., Bergstrom, D.A., and Tapscott, S.J. (1997). Two domains of MyoD mediate transcriptional activation of genes in repressive chromatin: a mechanism for lineage determination in myogenesis. Genes Dev. *11*, 436–450.

Heintzman, N.D., Hon, G.C., Hawkins, R.D., Kheradpour, P., Stark, A., Harp, L.F., Ye, Z., Lee, L.K., Stuart, R.K., Ching, C.W., et al. (2009). Histone modifications at human enhancers reflect global cell-type-specific gene expression. Nature *459*, 108–112.

Heinz, S., Benner, C., Spann, N., Bertolino, E., Lin, Y.C., Laslo, P., Cheng, J.X., Murre, C., Singh, H., and Glass, C.K. (2010). Simple combinations of lineage-determining transcription factors prime cis-regulatory elements required for macrophage and B cell identities. Mol. Cell *38*, 576–589.

Huang, W., Sherman, B.T., and Lempicki, R.A. (2009a). Bioinformatics enrichment tools: paths toward the comprehensive functional analysis of large gene lists. Nucleic Acids Res. *37*, 1–13.

Huang, W., Sherman, B.T., and Lempicki, R.A. (2009b). Systematic and integrative analysis of large gene lists using DAVID bioinformatics resources. Nat. Protoc. *4*, 44–57.

Hussey, K.M., Chen, H., Yang, C., Park, E., Hah, N., Erdjument-Bromage, H., Tempst, P., Gamble, M.J., and Kraus, W.L. (2014). The histone variant MacroH2A1 regulates target gene expression in part by recruiting the transcriptional coregulator PELP1. Mol. Cell. Biol. *34*, 2437–2449.

Iwafuchi-Doi, M., and Zaret, K.S. (2014). Pioneer transcription factors in cell reprogramming. Genes Dev. *28*, 2679–2692.

Jenuwein, T., and Allis, C.D. (2001). Translating the histone code. Science *293*, 1074–1080.

Jin, C., and Felsenfeld, G. (2007). Nucleosome stability mediated by histone variants H3.3 and H2A.Z. Genes Dev. *21*, 1519–1529.

Jin, C., Zang, C., Wei, G., Cui, K., Peng, W., Zhao, K., and Felsenfeld, G. (2009). H3.3/H2A.Z double variant-containing nucleosomes mark 'nucleosome-free regions' of active promoters and other regulatory regions. Nat. Genet. *41*, 941–945.

Kapoor, A., Goldberg, M.S., Cumberland, L.K., Ratnakumar, K., Segura, M.F., Emanuel, P.O., Menendez, S., Vardabasso, C., Leroy, G., Vidal, C.I., et al. (2010). The histone variant macroH2A suppresses melanoma progression through regulation of CDK8. Nature *468*, 1105–1109.

Kundaje, A., Meuleman, W., Ernst, J., Bilenky, M., Yen, A., Heravi-Moussavi, A., Kheradpour, P., Zhang, Z., Wang, J., Ziller, M.J., et al.; Roadmap Epigenomics Consortium (2015). Integrative analysis of 111 reference human epigenomes. Nature *518*, 317–330.

Kustatscher, G., Hothorn, M., Pugieux, C., Scheffzek, K., and Ladurner, A.G. (2005). Splicing regulates NAD metabolite binding to histone macroH2A. Nat. Struct. Mol. Biol. *12*, 624–625.

Ladurner, A.G. (2003). Inactivating chromosomes: a macro domain that minimizes transcription. Mol. Cell *12*, 1–3.

Langmead, B., Trapnell, C., Pop, M., and Salzberg, S.L. (2009). Ultrafast and memory-efficient alignment of short DNA sequences to the human genome. Genome Biol. *10*, R25.

Magnani, L., Ballantyne, E.B., Zhang, X., and Lupien, M. (2011). PBX1 genomic pioneer function drives ERα signaling underlying progression in breast cancer. PLoS Genet. *7*, e1002368.

Maves, L., Waskiewicz, A.J., Paul, B., Cao, Y., Tyler, A., Moens, C.B., and Tapscott, S.J. (2007). Pbx homeodomain proteins direct Myod activity to promote fast-muscle differentiation. Development *134*, 3371–3382.

Maze, I., Noh, K.M., Soshnev, A.A., and Allis, C.D. (2014). Every amino acid matters: essential contributions of histone variants to mammalian development and disease. Nat. Rev. Genet. *15*, 259–271.

Métivier, R., Penot, G., Hübner, M.R., Reid, G., Brand, H., Kos, M., and Gannon, F. (2003). Estrogen receptor-alpha directs ordered, cyclical, and combinatorial recruitment of cofactors on a natural target promoter. Cell *115*, 751–763.

Mootha, V.K., Lindgren, C.M., Eriksson, K.F., Subramanian, A., Sihag, S., Lehar, J., Puigserver, P., Carlsson, E., Ridderstråle, M., Laurila, E., et al. (2003). PGC-1alpha-responsive genes involved in oxidative phosphorylation are coordinately downregulated in human diabetes. Nat. Genet. *34*, 267–273.

Mousavi, K., Zare, H., Wang, A.H., and Sartorelli, V. (2012). Polycomb protein Ezh1 promotes RNA polymerase II elongation. Mol. Cell *45*, 255–262.

Mousavi, K., Zare, H., Dell'orso, S., Grontved, L., Gutierrez-Cruz, G., Derfoul, A., Hager, G.L., and Sartorelli, V. (2013). eRNAs promote transcription by establishing chromatin accessibility at defined genomic loci. Mol. Cell *51*, 606–617.

Pasque, V., Gillich, A., Garrett, N., and Gurdon, J.B. (2011). Histone variant macroH2A confers resistance to nuclear reprogramming. EMBO J. *30*, 2373–2387.

Pehrson, J.R., and Fried, V.A. (1992). MacroH2A, a core histone containing a large nonhistone region. Science *257*, 1398–1400.

Podrini, C., Koffas, A., Chokshi, S., Vinciguerra, M., Lelliott, C.J., White, J.K., Adissu, H.A., Williams, R., and Greco, A. (2014). MacroH2A1 isoforms are associated with epigenetic markers for activation of lipogenic genes in fat-induced steatosis. FASEB J. *29*, 1676–1687.

Quinlan, A.R., and Hall, I.M. (2010). BEDTools: a flexible suite of utilities for comparing genomic features. Bioinformatics *26*, 841–842.

Rada-Iglesias, A., Bajpai, R., Swigut, T., Brugmann, S.A., Flynn, R.A., and Wysocka, J. (2011). A unique chromatin signature uncovers early developmental enhancers in humans. Nature *470*, 279–283.

Ramakrishnan, V., Finch, J.T., Graziano, V., Lee, P.L., and Sweet, R.M. (1993). Crystal structure of globular domain of histone H5 and its implications for nucleosome binding. Nature *362*, 219–223.

Rasmussen, T.P., Huang, T., Mastrangelo, M.A., Loring, J., Panning, B., and Jaenisch, R. (1999). Messenger RNAs encoding mouse histone macroH2A1 isoforms are expressed at similar levels in male and female cells and result from alternative splicing. Nucleic Acids Res. *27*, 3685–3689.

Ratnakumar, K., Duarte, L.F., LeRoy, G., Hasson, D., Smeets, D., Vardabasso, C., Bönisch, C., Zeng, T., Xiang, B., Zhang, D.Y., et al. (2012). ATRX-mediated chromatin association of histone variant macroH2A1 regulates α-globin expression. Genes Dev. *26*, 433–438.

Skene, P.J., and Henikoff, S. (2013). Histone variants in pluripotency and disease. Development *140*, 2513–2524.

Soufi, A., Garcia, M.F., Jaroszewicz, A., Osman, N., Pellegrini, M., and Zaret, K.S. (2015). Pioneer transcription factors target partial DNA motifs on nucleosomes to initiate reprogramming. Cell *161*, 555–568.

Subramanian, A., Tamayo, P., Mootha, V.K., Mukherjee, S., Ebert, B.L., Gillette, M.A., Paulovich, A., Pomeroy, S.L., Golub, T.R., Lander, E.S., and Mesirov, J.P. (2005). Gene set enrichment analysis: a knowledge-based approach for interpreting genome-wide expression profiles. Proc. Natl. Acad. Sci. USA *102*, 15545–15550.

Tapscott, S.J. (2005). The circuitry of a master switch: Myod and the regulation of skeletal muscle gene transcription. Development *132*, 2685–2695.

Trapnell, C., Pachter, L., and Salzberg, S.L. (2009). TopHat: discovering splice junctions with RNA-Seq. Bioinformatics *25*, 1105–1111.

Trapnell, C., Hendrickson, D.G., Sauvageau, M., Goff, L., Rinn, J.L., and Pachter, L. (2013). Differential analysis of gene regulation at transcript resolution with RNA-seq. Nat. Biotechnol. *31*, 46–53.

Whyte, W.A., Orlando, D.A., Hnisz, D., Abraham, B.J., Lin, C.Y., Kagey, M.H., Rahl, P.B., Lee, T.I., and Young, R.A. (2013). Master transcription factors and mediator establish super-enhancers at key cell identity genes. Cell *153*, 307–319.

Yaffe, D., and Saxel, O. (1977). Serial passaging and differentiation of myogenic cells isolated from dystrophic mouse muscle. Nature *270*, 725–727.

Zang, C., Schones, D.E., Zeng, C., Cui, K., Zhao, K., and Peng, W. (2009). A clustering approach for identification of enriched domains from histone modification ChIP-Seq data. Bioinformatics *25*, 1952–1958.

Zaret, K.S., and Carroll, J.S. (2011). Pioneer transcription factors: establishing competence for gene expression. Genes Dev. *25*, 2227–2241.

Zentner, G.E., Tesar, P.J., and Scacheri, P.C. (2011). Epigenetic signatures distinguish multiple classes of enhancers with distinct cellular functions. Genome Res. *21*, 1273–1283.

Zhang, Y., Liu, T., Meyer, C.A., Eeckhoute, J., Johnson, D.S., Bernstein, B.E., Nusbaum, C., Myers, R.M., Brown, M., Li, W., and Liu, X.S. (2008). Model-based analysis of ChIP-Seq (MACS). Genome Biol. *9*, R137.